Data in Brief 47 (2023) 108928

Contents lists available at ScienceDirect

Data in Brief

journal homepage: www.elsevier.com/locate/dib

Data Article

Data for assessing red blood cell deformability from microscopy images using deep learning

Erik S. Lamoureux[a,b], Emel Islamzada[b,c], Matthew V.J. Wiens[d], Kerryn Matthews[a,b], Simon P. Duffy[a,b,e], Hongshen Ma[a,b,d,f,*]

[a] *Department of Mechanical Engineering, University of British Columbia, 2054-6250 Applied Science Lane, Vancouver, BC V6T 1Z4, Canada*
[b] *Centre for Blood Research, University of British Columbia, 4th Floor, 2350 Health Sciences Mall, Vancouver, BC V6T 1Z3, Canada*
[c] *Department of Pathology and Laboratory Medicine, University of British Columbia, 105-2211 Wesbrook Mall, Vancouver, BC V6T 2B5, Canada*
[d] *School of Biomedical Engineering, University of British Columbia, 2222 Health Sciences Mall, Vancouver, BC V6T 1Z3, Canada*
[e] *British Columbia Institute of Technology, 3700 Willingdon Ave, Burnaby, BC V5G 3H2, Canada*
[f] *Vancouver Prostate Centre, Vancouver General Hospital, 2660 Oak Street, Vancouver, BC V6H 3Z6, Canada*

ARTICLE INFO

Article history:
Received 29 July 2022
Revised 13 January 2023
Accepted 18 January 2023
Available online 25 January 2023

Dataset link: Data for: Assessing Red Blood Cell Deformability from Microscopy Images Using Deep Learning (Original data)

Keywords:
Red blood cells
Deformability
Microfluidics
Optical microscopy
Dataset
Computer vision
Machine learning
Deep learning

ABSTRACT

Red blood cell (RBC) deformability is a vital biophysical property that dictates the ability of these cells to repeatedly squeeze through small capillaries in the microvasculature. This capability is known to differ between individuals and degrades due to natural aging, pathology, and cold storage. There is great interest in measuring RBC deformability because this parameter is a potential biomarker of RBC quality for use in blood transfusions. Measuring this property from microscopy images would greatly reduce the effort required to acquire this information, as well as improve standardization across different centers. This dataset consists of live cell microscopy images of RBC samples from 10 healthy donors. Each RBC sample is sorted into fractions based on deformability using the microfluidic ratchet device. Each deformability fraction is imaged in microwell plates using a Nikon CFI S Plan Fluor ELWD 40 × objective and a Nikon DS-Qi2 CMOS camera on a Nikon Ti-2E inverted microscope. This

* Corresponding author.
E-mail address: hongma@mech.ubc.ca (H. Ma).

https://doi.org/10.1016/j.dib.2023.108928

data could be reused to develop deep learning algorithms to associate live cell images with cell deformability.

Specifications Table

Subject	Biomedical Engineering
Specific subject area	Single cell image analysis using deep learning
Type of data	2424 × 2424 pixel 8-bit greyscale images
How the data were acquired	The data was acquired using a Nikon Ti-2E inverted microscope configured for brightfield imaging with a Nikon CFI S Plan Fluor ELWD 40 × objective and a Nikon DS-Qi2 CMOS camera.
Data format	All images are 8-bit greyscale bitmaps. The raw image data are full microwell image scans. The cleaned image data excluded images outside the microwell or those that had poor focus.
Description of data collection	Self-identified healthy donors between the ages of 18–70 provided fresh or stored RBCs. These blood samples were sorted based on deformability using the microfluidic ratchet device. After sorting, the sorted cells were extracted and imaged. The imaging data were cleaned by removing images outside the well, as well as images with poor focus.
Data source location	Institution: University of British Columbia City/Town/Region: Vancouver, British Columbia Country: Canada Latitude and longitude (and GPS coordinates, if possible) for collected samples/data: 49.2606° N, 123.2460° W
Data accessibility	Repository name: Federated Research Data Repository Direct URL to data: https://doi.org/10.20383/103.0589
Related research article	Lamoureux, E. S., Islamzada, E., Wiens, M. V., Matthews, K., Duffy, S. P., & Ma, H. (2022). Assessing red blood cell deformability from microscopy images using deep learning. Lab on a Chip, 22(1), 26-39. https://doi.org/10.1039/D1LC01006A [1]

Value of the Data

- This dataset will be useful to researchers developing new AI algorithms to estimate RBC deformability from single cell images.
- Measuring RBC deformability is a technically challenging and time-consuming process that requires specialized equipment and personnel. Assessing RBC deformability from microscopy images would greatly reduce the amount of effort required to acquire this data and standardize this measurement across different centers.
- This dataset includes microscopy images of RBC samples from 10 donors. Each sample is sorted into fractions based on deformability.
- This dataset could be used to develop image analysis algorithms to associate RBC images with deformability, and importantly, to generalize this analysis across donors.
- This dataset can also be used to develop algorithms to segment single cells from microscopy images.

1. Data Description

This dataset consists of microscopy images of RBC samples from 10 donors who self-identified as healthy between the ages of 18-70. The RBCs were collected in citrate tubes (n = 4) or in blood bags (n = 6). Some of the RBC samples were imaged immediately after collection

Table 1
Number of images for each donor. The higher numbered outlets contain more rigid cells. Samples of sorted cells were split and imaged in two separate wells.

	Outlet 2		Outlet 3		Outlet 4		Outlet 5		Unsorted	
Donor	Well 1	Well 2	Well 1	Well 2	Well 1	Well 2	Well 1	Well 2	Well 1	Well 2
1	-	-	124	129	108	70	-	-	-	-
2	86	93	66	92	75	91	-	-	82	-
3	79	90	81	79	80	82	100	119	77	88
4	-	-	92	103	69	104	87	102	70	74
5	-	-	90	94	102	86	-	-	-	-
6	98	94	124	100	99	116	92	98	-	-
7	-	-	107	107	102	102	132	145	-	-
8	82	133	102	128	118	96	119	87	-	-
9	-	-	123	113	119	123	-	-	-	-
10	-	-	121	101	109	117	113	107	-	-

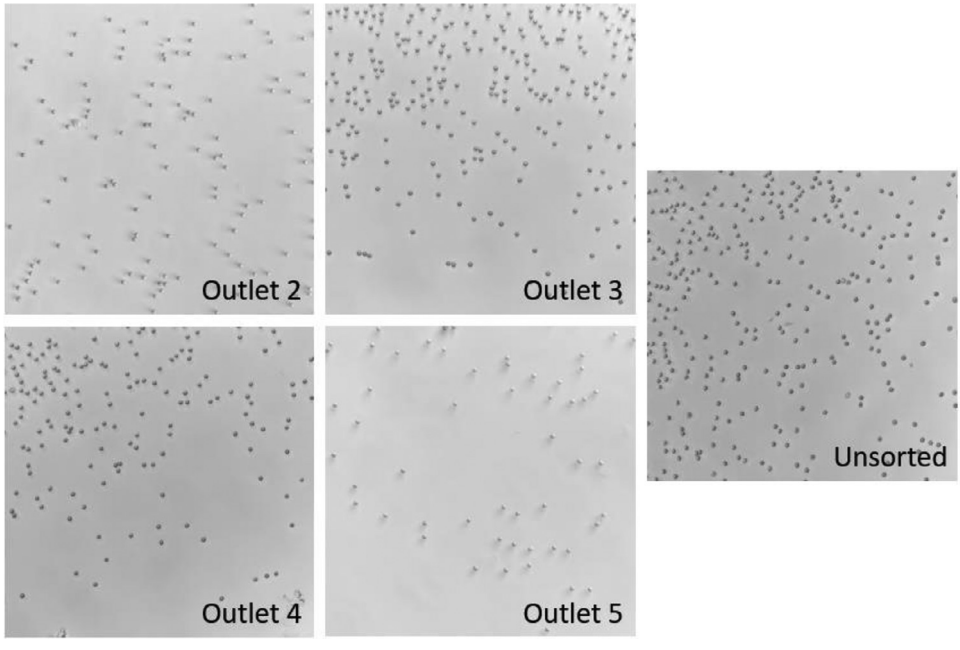

Fig. 1. Example 2424 × 2424 pixel bitmap raw images from donor 3.

(n = 3), one was imaged after storage in a plastic test tube at 4°C (n = 1), while others were stored in blood bags at 4°C (n = 6). The donors were diverse in terms of blood type and sex [1].

The microscopy image data consists of 6,491 grey-scale bitmap images of 2424 × 2424 pixels at 8-bit depth. For the 10 donors, each consists of sets of images for multiple deformability outlets (Table 1), where lower numbered outlets correspond to more deformable cells. Fig. 1 depicts example microscopy image from donor 3 including sorted (outlets 2-5) and unsorted cell images. Fig. 2 depicts the resultant images after preprocessing for single-cell image segmentation.

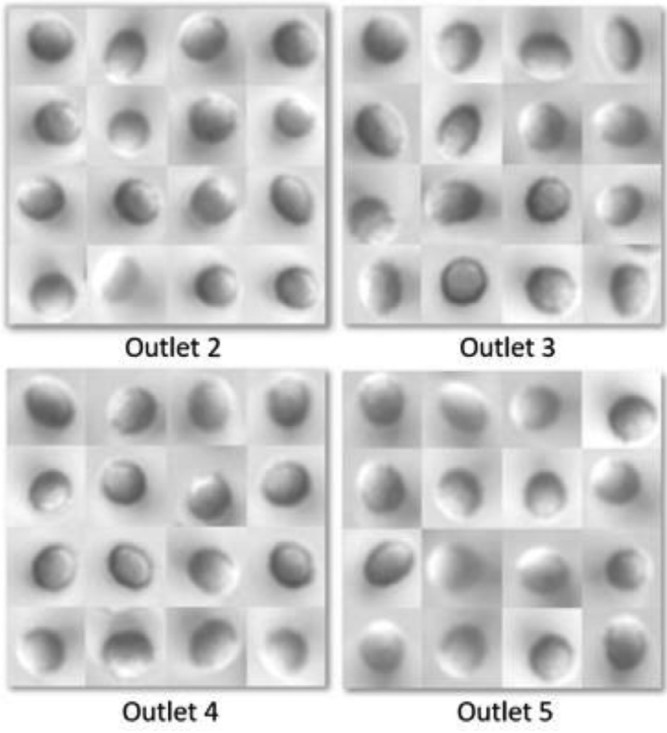

Fig. 2. Example preprocessed single-cell segmented images from donor 6. The images were segmented into single-cell images and augmented *via* rotation.

2. Experimental Design, Materials and Methods

2.1. Data collection

Donor whole blood samples were separated into components *via* centrifugation at 3180*g* for 8 minutes. Blood supernatant (plasma and white blood cells) were removed and discarded. The remaining red blood cell pellet was resuspended and washed three times in a five-fold dilution of Hanks balanced salt solution (HBSS, Gibco) with 0.2% Pluronic solution (F127, MilliporeSigma). Finally, the washed RBC pellet was resuspended in HBSS + 0.2% Pluronic at 1% hematocrit for infusion into the microfluidic ratchet sorting device.

The manufacture of the microfluidic devices has been described previously [2,3]. Briefly, a master mold was manufactured using photolithographic microfabrication and was used to fabricate a secondary master polyurethane mold [4]. From the secondary master molds, single-use microfluidic devices were fabricated using PDMS silicone (Sylgard-184, Ellsworth Adhesives). After the PDMS mold devices cured, they were punched with 0.5- and 3.0-mm hole punches to create the inlets and outlets, respectively. The 0.5-mm inlets were washed with deionized water for 15 seconds to remove any remaining PDMS debris. A thin PDMS layer (RTV 615, Momentive Performance Materials LLC) was produced by spinning uncured PDMS on a 100 mm silicon wafer. After curing, the thin PDMS layer was bonded to the molded PDMS device to seal its microstructures using air plasma. The resulting sealed microstructure molded device was bonded to a glass slide (Corning) using air plasma to allow for microscopy imaging.

The microfluidic device operates using microscale funnel constrictions to measure cell deformability. The operation of the microfluidic device has been described and validated previously

[5,6]. Four pressurized fluidic inputs operate the microfluidic ratchet sorting. Three of these inputs push HBSS + 0.2% Pluronic buffer fluid: first, a horizontal crossflow moves the RBC sample towards the outlets, and a coupled oscillating up-down pressure system squeezes cells through progressively smaller tapered constrictions and declogs other cells unable to pass through. Cells that squeeze through a minimum constriction size of 2.50 µm wide travel to outlet 5, 2.25 µm to outlet 4, 2.00 µm to outlet 3, and 1.75 µm to outlet 2. The fourth and final pressurized input pushes the 1% hematocrit sample into the microfluidic matrix sorting region. Running the device for 60-90 minutes will sort >30,000 cells into the outlets.

After cell sorting, cells were extracted from the microfluidic device and transferred into an imaging well plate. Each deformability outlet sample was split in two, producing two wells for imaging, allowing us to account for potential well-specific imaging bias (e.g., cell location shading bias). Full well image scans were conducted in brightfield using a Nikon CFI S Plan Fluor ELWD 40 × objective and a Nikon DS-Qi2 CMOS camera on a Nikon Ti-2E inverted microscope with NIS Elements software. A description of the raw data is found in the "Data description" section.

2.2. Data cleaning

The raw images were cleaned in several ways. First, the images were manually audited to remove images captured outside the microwell or that were out of focus. The remaining images after this manual audit are included in the referenced data repository for this work [7]. To make these images useful for deep learning classification, a computer vision algorithm was used to extract single-cell images of size 60 × 60 pixels. The code used to segment the cells can be found here [8]. After single cell segmentation, each image was manually reviewed to remove those with no cells, partial cells, multiple cells, or those that were out of focus. The resulting cleaned dataset was further processed. Images from well 1 and well 2 from each outlet for a specified donor were combined to increase the variations within the deformability class. From this, we split the images 80/20 from each outlet to produce separate sets for training and testing. Since most cells (∼80%) were sorted to outlets 3 and 4, we decided to split the deformability groups into *deformable* (outlets 2 and 3) and *rigid* (outlets 4 and 5) classes. After train-test splitting and combining the outlets, we introduced further image variation using an image augmentation protocol to rotate single-cell images by a random integer multiple of 90°. This method produced 10,000 images for training and 2,000 images for testing for each deformability class. This augmentation approach is presented in our Github repository [8].

2.3. Analysis

The balanced datasets were used to train a convolutional neural network (CNN) model for binary deformability classification for each donor. Our CNN model design can be found here [1] and was influenced by the AlexNet model architecture [9] and other deep learning architecture used in our lab [10]. The model was implemented in Python 3.7 using the Keras library in TensorFlow. For feature extraction, the model used a series of 4 convolutional layers (sequential kernel sizes of 7 × 7, 5 × 5, 3 × 3, and 3 × 3) and 3 max pooling layers. Each convolutional layer was followed by batch normalization and ReLU activation. Then, the 3 fully connected layers were followed by batch normalization, ReLU activation, and 20% dropout. The output layer used a SoftMax error function for backpropagation during training. We used a binary cross-entropy loss function and stochastic gradient descent for optimization. The implementation of this model can be found here [8].

The model was trained and validated using five-fold cross validation. We iteratively determined optimal donor-specific learning rates and number of epochs, ranging from 0.0001 to 0.1 and 25 to 80, respectively. A stochastic gradient descent operator was reliable across the 10

donors and was used with decay 10^{-6} and Nesterov momentum 0.9. A batch-size of 32 was held for all donors.

After training and testing, the model's performance was assessed in multiple ways. First, we conducted saliency maps to assess whether the model was learning and classifying deformability based on relevant cell morphological features. Second, performance evaluations including confusion matrices, accuracy, precision, recall, F1-score, ROC AUC were performed. Finally, the deep-learning derived donor deformability score was compared to the microfluidic-derived score [1].

This dataset provides a comprehensive group of images at varying deformability levels for 10 donors who are diverse in terms of age, sex, and blood type. By further refining and developing deep learning platforms to assess red blood cell deformability, there is potential to alleviate the technical and equipment burdens associated with cell deformability measurement. Ultimately, this capability could enable blood banks to routinely assess RBC deformability in order to assess the quality of donated red blood cell units.

Ethics Statements

This study was approved by the University of British Columbia's Clinical Research Ethics Board (UBC REB# H19-01121) and Canadian Blood Services Research Ethics Board (CBS REB# 2019-029).

Declaration of Competing Interest

H. M. is listed as an inventor on a patent related to this work.

Data Availability

Data for: Assessing Red Blood Cell Deformability from Microscopy Images Using Deep Learning (Original data) (Federated Research Data Repository).

CRediT Author Statement

Erik S. Lamoureux: Conceptualization, Methodology, Investigation, Software, Writing – original draft; **Emel Islamzada:** Investigation; **Matthew V.J. Wiens:** Software; **Kerryn Matthews:** Investigation; **Simon P. Duffy:** Conceptualization, Writing – review & editing; **Hongshen Ma:** Supervision, Conceptualization, Writing – review & editing.

Acknowledgments

We are grateful to Canadian Blood Services' blood donors who made this research possible.

This work was supported by grants from the Canadian Institutes of Health Research (322375, 362500, 414861), Natural Sciences and Engineering Research Council of Canada (538818-19, 2015-06541), MITACS (K. M. IT09621), and the Canadian Blood Services Graduate Fellowship Program (E. I.), which is funded by the federal government (Health Canada) and the provincial and territorial ministries of health. The views herein do not necessarily reflect the views of Canadian Blood Services or the federal, provincial, or territorial governments of Canada.

References

[1] E.S. Lamoureux, E. Islamzada, M.V.J. Wiens, K. Matthews, S.P. Duffy, H. Ma, Assessing red blood cell deformability from microscopy images using deep learning, Lab. Chip 22 (1) (2022) 26–39, doi:10.1039/D1LC01006A.

[2] Q. Guo, et al., Deformability based sorting of red blood cells improves diagnostic sensitivity for malaria caused by Plasmodium falciparum, Lab. Chip 16 (4) (2016) 645–654, doi:10.1039/C5LC01248A.

[3] Q. Guo, S.P. Duffy, K. Matthews, E. Islamzada, H. Ma, Deformability based cell sorting using microfluidic ratchets enabling phenotypic separation of leukocytes directly from whole blood, Sci. Rep. 7 (1) (Dec. 2017) 6627, doi:10.1038/s41598-017-06865-x.

[4] S.P. Desai, D.M. Freeman, J. Voldman, Plastic masters—rigid templates for soft lithography, Lab. Chip 9 (11) (2009) 1631, doi:10.1039/b822081f.

[5] Q. Guo, S. Park, H. Ma, Microfluidic micropipette aspiration for measuring the deformability of single cells, Lab. Chip 12 (15) (2012) 2687, doi:10.1039/c2lc40205j.

[6] E. Islamzada, et al., Deformability based sorting of stored red blood cells reveals donor-dependent aging curves, Lab. Chip 20 (2) (2020) 226–235, doi:10.1039/C9LC01058K.

[7] E.S. Lamoureux, E. Islamzada, M.V.J. Wiens, K. Matthews, S.P. Duffy, H. Ma, Data for: Assessing Red Blood Cell Deformability from Microscopy Images Using Deep Learning, Federated Research Data Repository, 2022 [Online]. Available:, doi:10.20383/103.0589.

[8] E.S. Lamoureux, M.V.J. Wiens, Assessing Red Blood Cell Deformability using Deep Learning, Github, 2022. [Online]. Available:. https://github.com/lamoureuxe/Assessing-Red-Blood-Cell-Deformability-using-Deep-Learning .

[9] A. Krizhevsky, I. Sutskever, G.E. Hinton, ImageNet Classification with deep convolutional neural networks, in: F. Pereira, C.J.C. Burges, L. Bottou, K.Q. Weinberger (Eds.), Advances in Neural Information Processing Systems 25, Curran Associates, Inc., 2012, pp. 1097–1105. [Online]. Available: http://papers.nips.cc/paper/4824-imagenet-classification-with-deep-convolutional-neural-networks.pdf.

[10] S. Berryman, K. Matthews, J.H. Lee, S.P. Duffy, H. Ma, Image-based phenotyping of disaggregated cells using deep learning, Commun. Biol. 3 (1) (Dec. 2020) 674, doi:10.1038/s42003-020-01399-x.